

Preparation and in-vitro Applications of Doxorubicin Loaded on Functionalized Multi-walled Carbon Nanotubes

El-Shahat A. Toson^{*1}, Norhan A. Rezk¹ and Rasha F. Zahran¹

¹Chemistry Department, Faculty of Science, Damietta University, New Damietta City, Egypt.

Received: 23 March 2023 /Accepted: 13 April 2023

* Corresponding author's E-mail: eatoson@yahoo.com

Abstract

One of the most crucial nanomaterials used in applications of biomedicine is Multi-Walled Carbon nanotubes (MWCNTs). It is applicable in delivering of different drugs to the tumor target sites, including doxorubicin (DOX). This is because the functionalized MWCNTs can penetrate membranes with low cytotoxicity. In this study, MWCNTs were oxidized (Ox-MWCNTs) to improve their solubility and biocompatibility. Their abilities to encapsulate DOX were tested (Ox-MWCNT/DOX). These particles were then characterized using FTIR, TEM, SEM and zeta size. Their antitumor activities against *in-vitro* MCF-7 and NBL cells were estimated. The results of FTIR confirmed the addition of carboxyl groups to the MWCNTs followed by encapsulation of DOX. Their shape was tubular with open ends using TEM. From their surface view, SEM showed the tubes as hollow spheres with interconnected structure. Higher releasing rate of DOX at pH 5.8 comparing with pH 7.4 was observed. Treating of human breast cancer cells (MCF-7) with Ox-MWCNT/DOX resulted in cellular viabilities of 96 ± 0.37 , 87 ± 0.7 , 34.7 ± 0.75 , 14.3 ± 1 and 4.2 ± 0.5 % at doses equivalent to 0.1, 1, 10, 100 and 1000 $\mu\text{g/ml}$ free DOX, respectively. Moreover, higher viabilities (99.8 ± 0.13 , 99.54 ± 0.69 , 77.42 ± 1.13 , 62.48 ± 0.1 and 55.3 ± 1.25 %) with lower cytotoxicities of normal liver cells (NBL) were observed under the same treatment protocol. Therefore, the investigated loading protocol may be a promising one for the treatment of such tumor type after further studies in the future.

Keywords: Carbon nanotubes, Doxorubicin, Drug delivery system, Cytotoxicity.

Introduction

Chemotherapy, as with doxorubicin, is one of the most-applicable treatments of cancer. However, these anticancer drugs cause severe side effects (Wang *et al.*, 2018). The reason may extrapolate to their inability to

distinguish accurately between tumor cells and normal ones (Rivankar 2014). The mechanisms are based on inhibition of the fast proliferation of cancer cells. Unfortunately, they also inhibit the fast growth needed for the maintenance of bone marrow, and other cells (Sheikhpour *et al.*, 2017). With a final effect on the life quality of the patients. In order to resolve this issue, nano-carriers were used to

sustainably deliver these chemotherapeutic drugs to the tumor sites (**Rivankar 2014**).

In this regard, MWCNTs has recently attracted significant attention for the use in targeted drug delivery. This is mostly as a result of their hollow tubular structure, ultrahigh surface area (up to 1700 m²/g) and their abilities to cross cell membranes via perpendicular positioning exactly as that of nano-needles (**Qi et al., 2015; Elhissi et al., 2011**)

In order to establish MWCNTs in potential DOX drug delivery, they must be functionalized (**Jain et al., 2022**). The functionalized MWCNTs are complete graphene regions that are interspersed with sp²-hybridized carbon that contains hydroxyl, epoxide and carboxylic groups which are able to form π - π interaction with quinone fragment of DOX. Also, the DOX amino and hydroxyl groups can react with the hydroxyl and carboxylic groups of the functionalized MWCNTs via hydrogen-bonds (**Carvalho et al., 2009**). In preclinical models, it has been reported that such encapsulation protocol of DOX leads to a 35-fold increase in the experimental animals' half-life times due to a 10-fold increase in drug accumulation at the tumor site (**Wang et al., 2018**).

Materials

MWCNTs' diameter equal 9.5 nm and length equal 1.5 μ m were procured from Sigma Aldrich, Doxorubicin HCl (2mg/ml) was procured from a local pharmacy. Other chemicals and reagents of the highest available pure grade were used.

Methods

Nanoparticles preparation

Purification of pristine MWCNTs

Ten mg of MWCNTs were suspended in 5ml of ethanol. This solution was then sonicated for 30 mins to disperse its components. Then, the solution was filtrated by using 0.45 μ m filter membrane and the precipitate was dried at 100 °C for one hr.

Oxidation of MCNTS

One mg of the purified MWCNTs were dispersed in 1 ml mix of concentrated sulfuric and nitric acids (3:1 V/V). Then, the dispersed solution was sonicated for 4hr at 40°C. The previous solution was then filtrated by using 0.45 μ m filter membrane. Distilled water was used for washing the precipitate until neutralization point of filtrate was reached. After that, the functionalized MWCNTs were dried at 60°C. The oxidation product is termed oxidized multi-walled carbon nanotubes (OX-MWCNTs).

Loading DOX on Ox-MWCNTs

One mg of Ox-MWCNTs were dispersed in 5mL of distilled water and sonicated for 5 minutes before adding 1 mL of DOX and completing with distilled water to a volume of 9mL. Then, the pH was adjusted to 8 and stirred for 24hr in the darkness at 25°C. The mixture was filtrated by using 0.45 μ m filter membrane and the precipitate was washed by distilled water till the color of DOX disappear and the filtrate became colorless. This was confirmed by absence of the absorbance at 481nm. The Ox-MWCNTs/DOX was dried and stored at 5°C till use.

Drug loading percentage and its loading efficiency had been calculated from calibration curve of DOX.

Evaluation of DOX loading efficiency:

The following equation was used to estimate the loading efficiency of DOX spectrophotometrically:

$$\text{Loading efficiency} = (S_1/S_0) * 100\%$$

$$\text{Loading percentage} = (S_1/(S_1+S_2)) * 100$$

Were:

S₀ is initial weight of DOX, S₁ is loaded DOX weight and S₂ is MWCNTs weight.

In-vitro release of drug

Releasing DOX from nanotubes was evaluated *in vitro* in acetate buffer (pH 5.8 and 6.2) and PBS of pH 7.4. from ox-MWCNTs was evaluated *in vitro* in PBS (pH 7.4) and acetate buffer (pH 5.8 and 6.2). Ox-MWCNTs/ DOX were dispersed in 4 mL of the selected buffer in dialysis bags with cut of molecular weight (MWCO) 12:14 kDa. The bags were submerged

in 10 ml of the corresponding buffer. These dialysis bags were kept in the dark at 37°C. The released amount of DOX was calculated at interval times through taking 1ml aliquots and the absorbance was measured at 481nm in each case.

Release percentage (%)= (amount of DOX released/total amount of loaded DOX) *100

Characterization of nanoparticles:

Fourier transform infrared (FTIR) spectroscopy

FTIR (Jasco, Easton,MD,USA) spectra of Ox-MWNTs and Ox-MWNTs/DOX were done to determine the chemical structure and to study the reactions between Ox-MWCNTs and DOX. In summary, FTIR samples were equipped by grinding 89.9% potassium bromide with 1.1% nanoparticles followed by demanding this mixture to a transparently pallet. The range of scanning resolution is (400-4000) cm⁻¹ (**Chanphai et al., 2019**).

Transmission electron microscopy (TEM)

The MWCNT samples' size and surface morphology were examined using transmission electron microscopy (TEM) (JSM-1230 EX II, JEOL, Tokyo, Japan). MWCNT Samples were equipped by putting drop of MWCNTs samples on a Cu grid. The remaining water was removed. After that, the micrographs were taken at a voltage accelerating 60 KV (**Kumari et al., 2018**).

Scanning electron microscope (SEM)

The samples were characterised for their morphological structure by scanning electronic microscope (SEM). 5mg of each MWCNTs sample was suspended in 1mL water using sonicator and put on an aluminum stump having a dual-stick tape of carbon. After that, the MWCNTs samples were dried and covered with Au under Ar atmosphere using a sputter coater. Samples were examined in high vacuum mode at 10 and 20 KV accelerating voltages. (**Kumari et al., 2018**).

Particle size and polydispersity

Size of nanotubes (nm) and their polydispersity index (PDI) were assessed using

dynamic light scattering (DLS) analysis for all the MWCNTs samples. Each sample of MWCNTs was examined after dilution for 50 times with deionized water and placed in disposable polystyrene cuvettes and the scatter intensity was measured at 25°C and repeated triplicate (**Wu et al., 2021**).

In-vitro assay of cytotoxicity

Cell culture:

Human breast cancer cell line (MCF-7 cells) and mouse normal liver cell line (BNL) were used in this study. These cells were purchased from Nawaht Scientific Inc., (Mokhatam, Cairo, Egypt). For 24 hours, the cells were cultured in RPMI media with supplementary 100 Units/mL penicillin, 100 mg/mL streptomycin, and 10% heat-inactivated foetal bovine serum in a moistened, 5% (V/V) CO₂ atmosphere at 37 °C.

Evaluation of cytotoxicity using viability assay:

The cytotoxicity of free DOX and Ox-MWCNTs/DOX were tested against MCF-7 cell line as well as NBL as normal cell line. The cells viabilities were assessed using SRB assay. 100µL of well shacked suspended cells (5x10³ cells) were pipetted in 96-well plates and incubated in complete media for 24hr. Another 100µL media including either free DOX or Ox-MWCNTs/ DOX at different concentrations were used for treating these cells. These concentrations were as follow: (0.1, 1,10,100,1000µg/ml). After 24hr of drug addition, media was replaced by10% TCA for fixation. The cells were then incubated at 4 °C for another hour. Decantation was used to remove the TCA-containing media. The cell pellets were washed with PBS of PH 7.4 several times. The cells were then incubated in a dark place at room temperature for 10 minutes with aliquots of 70L of SRB solution (0.4% w/v). The plates were then washed three times with 1% acetic acid and air-dried overnight. Then, 150L of Tris-buffer (10mM) was added to dissolve the protein-bound SRB stain. The absorbance of SRB was then measured at 540 nm with a BMG LABTECH®- FLUOstar Omega microplate reader (Ortenberg, Germany). The following equation was used to calculate the percentage of viability:

Cell viability (%) = $\text{Abs}_{\text{sample}}/\text{Abs}_{\text{control}} \times 100\%$
 where $\text{Abs}_{\text{sample}}$ was the absorbance for treated cells with the free and loaded DOX, while $\text{Abs}_{\text{control}}$ was the absorbance for the untreated cells.

In Vitro Flow Cytometric Analysis:

Cell culture

MCF-7 cell line was used in this study. These cells were purchased from Nawaht Scientific Inc., (Mokhatam, Cairo, Egypt). The cells were cultured in RPMI media with supplementary 100 units/mL penicillin, 100 mg/mL streptomycin, and 10% heat-inactivated foetal bovine serum in a humidified, 5% (V/V) CO₂ atmosphere at 37 °C for 24 hours.

Cell cycle analysis (propidium iodide assay):

Cell cycle distribution after treating cell line with free and loaded drug (at an equivalent dose to the free one) for 24 h were analyzed. 10⁵ MCF-7 cells were harvested by trypsinization. After that, they were washed twice with ice-cold PBS (pH 7.4). These cells were resuspended in two millilitres of 60% ice-cold ethanol and fixed for one hour at 4°C. After being washed twice with PBS (pH 7.4), the cells were resuspended in 2 mL of PBS containing 100 g/2mL RNAase and 20g/2mL propidium iodide (PI). After 20 minutes of incubation in the dark at 37 °C, cells were tested for DNA content using flow cytometry with the FL2 (ex/em 535/617 nm) signal detector. ACEA NovoExpress™ software was used to investigate cell cycle distribution.

Detection of apoptosis by Annexin V/PI dual staining:

The number of necrotic and apoptotic cells was determined using an Annexin V-FITC apoptosis detection kit (Abcam Inc., Cambridge Science Park, Cambridge, UK) in conjunction with two fluorescent channel flowcytometry. After 24 hours of treatment with free and loaded DOX, 10⁵ MCF-7 cells were trypsinized. These cells were washed with ice-cold PBS twice (pH 7.4). The cells were then incubated in the dark for 30 minutes at 25°C with 0.5 ml of Annexin V-FITC/PI according to the manufacturer's protocol. After staining, cells were injected into an ACEA Novocyte™ flowcytometer and

analysed for the presence of FITC and PI fluorescent signals using FL1 and FL2 signal detectors (ex/em 488/530 nm for FITC and ex/em 535/617 nm for PI). 12,000 events are generated for each sample, and positive FITC and/or PI cells are quantified using quadrant analysis and then calculated using ACEA NovoExpress™ software (ACEA Biosciences Inc., San Diego, CA, USA).

Statistical analysis:

Data were analyzed using SPSS software (version 22). All results were expressed as mean ± STD. The one-way ANOVA test was used to analyze the differences in means between the cell lines treated with loaded drug compared to the free one. The level of statistical significance was set at $p < 0.05$.

Results:

Characterization of OX- MWCNTs and OX- MWCNTs/DOX:

Fourier transform infrared (FTIR):

Functional groups of Ox-MWCNTs presence was confirmed by the FTIR spectrum as shown in figure 1. In this figure, the characteristic peak of C=O appeared at 1629 cm⁻¹ and the hydroxyl stretching of the carboxylic group of the Ox-MWCNTs appeared at 3437 cm⁻¹. Loading of DOX on Ox-MWCNTs nanotubes was confirmed by the appearance of the absorption bands at 974 cm⁻¹, 1258 cm⁻¹ and 1433 cm⁻¹ for OX-MWCNTs/DOX which are associated to the drug.

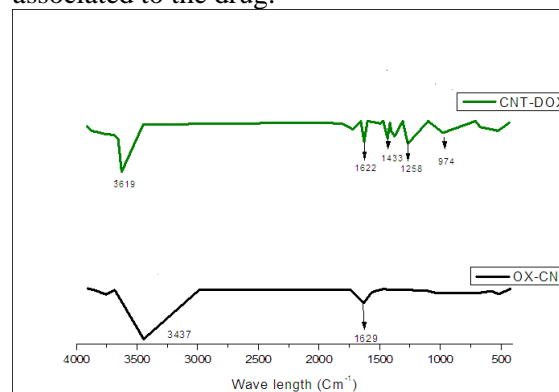


Figure 1: FTIR spectrum of OX-MWCNTs and OX-MWCNTs/DOX.

Transmission electron microscope (TEM):

As showed in **figure 2**, TEM was taken for each sample at two different magnifications to show the particle shape and surface morphology for samples. Ox-MWCNTs and OX-MWCNTS/DOX had shown a tubular shape with opening ends in Nano metric size. Furthermore, the images of OX-MWCNTS/DOX recommended that there was no difference in these tubular structure but became darker and had many smaller fragments. Also, when the Ox-MWCNTs were treated with DOX for longer periods with sonication and stirring, Ox-MWCNTs well dispersed and tended to be less aggregated in water.

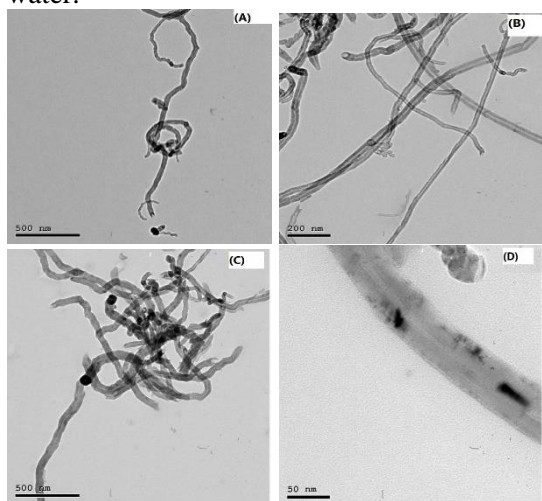


Figure 2: Photomicrograph of TEM for Ox-MWCNTs (A, B) and OX-MWCNTS/DOX (C, D).

Scanning electron microscope (SEM):

SEM was used for characterization of the produced nanotubes to confirm the loading of DOX. The nanoparticles of Ox-MWCNTs and those of OX-MWCNTS/DOX were tubular and appeared as hollow spherical structures with interconnected surface.

The morphological structure of OX-MWCNTS/DOX showed slightly change when compared to that of Ox-MWCNTs nanoparticles as it appeared more filled and darker than Ox-MWCNTs nanoparticles.

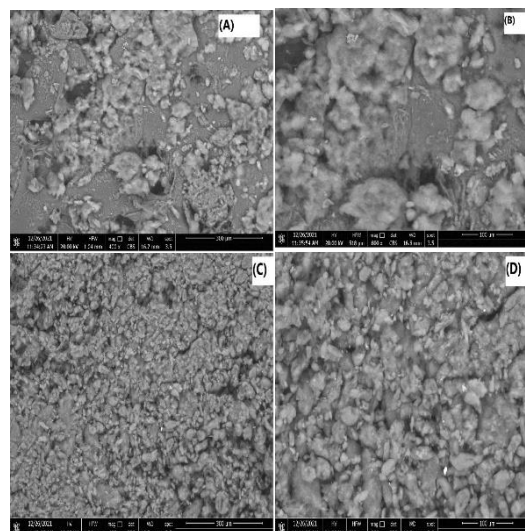


Figure 3: Photomicrograph showing SEM for Ox-MWCNTs (A, B) and OX-MWCNTS/DOX (C, D).

Particle Size and Zeta Potential:

The size of Ox-MWCNTs and OX-MWCNTS/DOX using DLS technique were depicted in **Figure 4**. In this figure the average size of the first nanoparticles is about 213 nm with polydispersity index (PDI) equal 0.233. Moreover, after the loading of DOX, the particles size of Ox-MWCNTs was increased as the average size reached 730 nm and with PDI of 0.321.

Figure (4B) shows the surface charge of Ox-MWCNTs which is -32.4.



Figure 4: Zeta potential and size of Ox-MWCNTs (A, B) and OX-MWCNTS/DOX(C).

DOX encapsulation and release study:

A 16.5% of DOX to Ox-MWCNTs (DLP) was used in this study while encapsulation efficiency (EE) was 89.86%. The release study was performed at 3 different pH values (5.8, 6.2, 7.4) at 37°C for 7 days as showed in **figure 5**. The results showed the drug release from OX-MWCNTS at pH 5.8 was more improved than at pH 7.4 and pH 6.2.

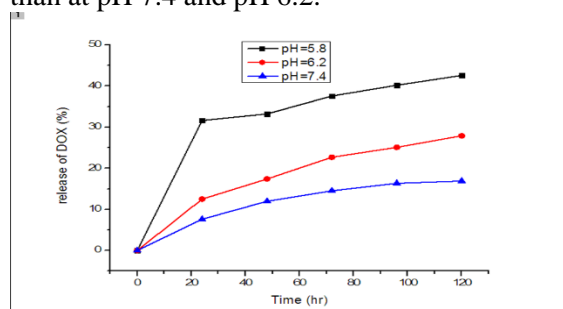


Figure5: In-vitro release of DOX and OX-MWCNTS/DOX at different pH values.

In vitro Cytotoxicity by Sulforhodamine B (SRB) Assay:

SRB (a bright-pink amino xanthene dye) binding assay was used to measure the cytotoxicity of free DOX and Ox-MWCNTs/DOX towards MCF-7 and NBL cell lines (figure 6, Table 1). Free DOX at concentrations range from 0.1 to 1000 g/ml improved cell cytotoxicity of NBL and MCF-7 cell lines in a dose manner dependent (5.53 and 10.94%), with respective viability results of 94.47 ± 0.51 and $89.06 \pm 1.197\%$. By increasing the concentration of DOX to 1000g/ml, the cell cytotoxicity of MCF-7 and NBL cell lines

increased to 94.93 ± 0.0099 and $99.48 \pm 0.045\%$ for NBL and MCF-7 cells, respectively, with respective viability results of 5.07 and 0.512%.

Ox-MWCNTs/DOX demonstrated a dose-dependent increase in cytotoxicity against MCF-7 at equivalent concentrations of free DOX. The maximum dose of Ox-MWCNTs/DOX, which was equivalent to 1000 g/ml of DOX, demonstrated 95.89% cytotoxicity and 4.11% cell viability. This cytotoxicity, on the other hand, is slightly lower than that of the free one.

Furthermore, treating NBL cell lines with Ox-MWCNTs/DOX at the same concentration as free DOX (0.1 g/ml) resulted in lower cytotoxicity ($0.2 \pm 0.087\%$) with comparison to free DOX. Furthermore, the viability of these cells was $99.8 \pm 0.13\%$. The higher dose of Ox-MWCNTs/DOX, equivalent to 1000 g/ml of DOX, had a lower toxicity than the free drug, with cell viability of $55.3 \pm 0.05\%$.

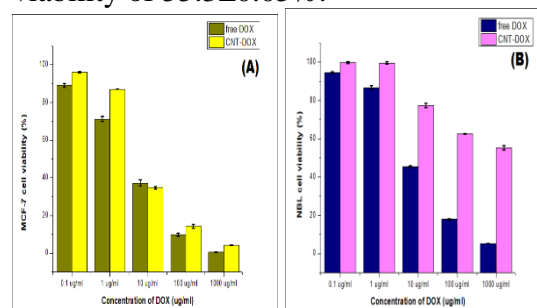


Figure6: Relative viabilities of MCF-7 (A) and NBL (B) cells after their incubation with 0.1,1,10,100,1000µg/ml of free DOX and loaded DOX for 24 hr.

Table 1: Mean±SD of cells viabilities treated with free and loaded DOX at different doses.

Dose (µg/ml)	NBL cell Viability(%)		MCF-7 cell Viability(%)	
	Free DOX	Loaded DOX	Free DOX	Loaded DOX
0.1	94.479 ± 0.519	99.7324 ± 0.575	89.0689 ± 1.07	96.039 ± 0.37
1	86.6351 ± 1.076	99.54 ± 0.692	71.1062 ± 1.35	87.0229 ± 0.06
10	45.3121 ± 0.411	77.4256 ± 1.137	37.2442 ± 1.6	34.6998 ± 0.75
100	17.961 ± 0.315	62.4875 ± 0.105	9.74875 ± 0.7	14.30167 ± 1
1000	5.1765 ± 0.00998	55.3 ± 1.25	0.52296 ± 0.03	4.212 ± 0.06

In vitro Flow Cytometry Analysis:

Cell Cycle analysis:

In vitro analysis of cell cycle was performed on MCF-7 cell lines treated with free DOX and Ox-MWCNTs/DOX. The flow cytometry

protocol was used to assess the population distribution of the different cell cycle phases based on their DNA content after staining with PI. Figure7 depicts the histogram plotting of these results. The cells treated with free DOX accumulated in the G1 phase at 45.62%, 30.11% in G2, 22.8% in S, and 1.47% in the

sub-G1 phase. Furthermore, cells treated with Ox-MWCNTs/DOX accumulated more in G1 with 49.85%, 23% in S, and less in G2 with 21.5% and 1.68 in the sub-G1 phase.

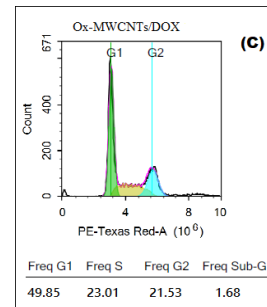
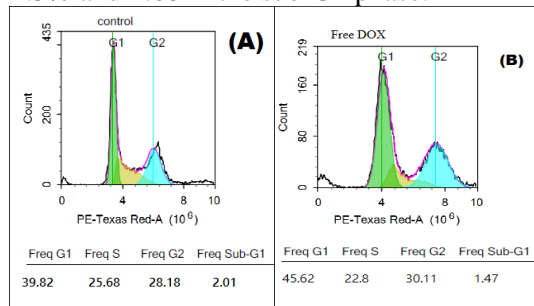


Figure 7: Histograms of Cell cycle of Control cells (A), treated cells with free DOX(B), treated cells with Ox-MWCNTs/DOX(C).

Table 2: Statistical results of NBL cell viabilities treated with loaded DOX compared to the free one at each dose.

	freeDOXdose1	freeDOXdose2	freeDOXdose3	freeDOXdose4	freeDOXdose5
Loaded DOXdose1					
r	-0.98 ⁿ	-1.00 ^s	-0.999 ^s	-0.567 ⁿ	0.999 ^s
p	0.127	0.014	0.022	0.616	0.033
Loaded DOXdose2					
r	0.979 ⁿ	1.00 ^s	0.999 ^s	0.57 ⁿ	-0.998 ^s
p	0.13	0.01	0.024	0.614	0.035
Loaded DOXdose3					
r	0.986 ⁿ	1.00 ^s	1 ^{sss}	0.538 ⁿ	-1 ^s
p	0.105	0.01	0.0001	0.638	0.011
Loaded DOXdose4					
r	0.984 ⁿ	1.00 ^{ss}	1 ^{ss}	0.548 ⁿ	-1 ^s
p	0.113	0.003	0.007	0.631	0.018
Loaded DOXdose5					
r	0.986 ⁿ	1.00 ^s	1 ^{sss}	0.538 ⁿ	-1 ^s
p	0.105	0.01	0.0001	0.638	0.011

As r: Pearson correlation, P: significance(2-tailed), and data are represented for loaded DOX comparing to free DOX at the five doses where Asterisks (s,ss,sss) indicates low significant, significant and highly significant, respectively while (n) not significant, dose1, 2, 3, 4 and 5 equal (0.1, 1, 10, 100 and 1000µg/ml).

Table3: Statistical results of MCF-7 cell viabilities treated with loaded DOX compared to the free one at each dose.

	freeDOXdose1	freeDOXdose2	freeDOXdose3	freeDOXdose4	freeDOXdose5
loadedDOXdose1					
r	0.266 ⁿ	-0.999 ^s	-0.91 ⁿ	0.978 ⁿ	0.67 ⁿ
P	0.829	0.033	0.273	0.133	0.532
loadedDOXdose2					
r	0.31 ⁿ	-0.995 ⁿ	-0.928 ⁿ	0.987 ⁿ	0.636 ⁿ
P	0.8	0.062	0.243	0.103	0.561
loadedDOXdose3					
r	-0.375 ⁿ	0.986 ⁿ	0.951 ⁿ	-0.996 ⁿ	-0.581 ⁿ
P	0.755	0.106	0.199	0.059	0.606
loadedDOXdose4					
r	0.37 ⁿ	-0.987 ⁿ	-0.95 ⁿ	0.995 ⁿ	0.585 ⁿ
P	0.759	0.103	0.203	0.063	0.602
loadedDOXdose5					
r	-0.372 ⁿ	0.987 ⁿ	0.951 ⁿ	-0.995 ⁿ	-0.583 ⁿ
P	0.757	0.104	0.201	0.061	0.604

As r: Pearson correlation, P: significance(2-tailed), and data are represented for loaded DOX comparing to free DOX at the five doses where Asterisks (s,ss,sss) indicates low significant, significant and highly significant, respectively while (n) not significant, dose1, 2, 3, 4 and 5 equal (0.1, 1, 10, 100 and 1000µg/ml)

Table 4: Percentage of cells distributions in different cell cycle phases

Phase	Control cells	Cells treated with free DOX	Cells treated with loaded DOX
G1	39.82±1.2	45.62±1.41 ^{ss1}	49.85±1.33 ^{sss1,s2}
S	25.68±0.97	22.8±0.88 ^{s1}	23.01±0.92 ^{s1,n2}
G2	28.18±0.91	30.11±0.69 ^{s1}	21.53±0.81 ^{ss1,ss2}
Sub G1	2.01±0.06	1.47±0.047 ⁿ¹	1.68±0.022 ^{n1,n2}

Data represented as mean±SD where, Asterisks (s,ss,sss) indicates low significant, significant and highly significant, respectively while (n) not significant,¹ comparing to control cells and ² comparing to cells treated with free DOX

Apoptosis analysis:

The extent of apoptosis induced by DOX in the free or loaded form was measured using an annexin V/PI double staining assay. The cell line treated with free DOX induced 9.36% total apoptosis (Q2+Q4) and 58.27% necrosis (Q1). The apoptotic and necrotic cell percentage, on the other hand, increased in cell lines treated with Ox-MWCNTs/DOX at equivalent concentrations of free DOX, reaching 13.6% for apoptosis and 60.04% for necrosis.

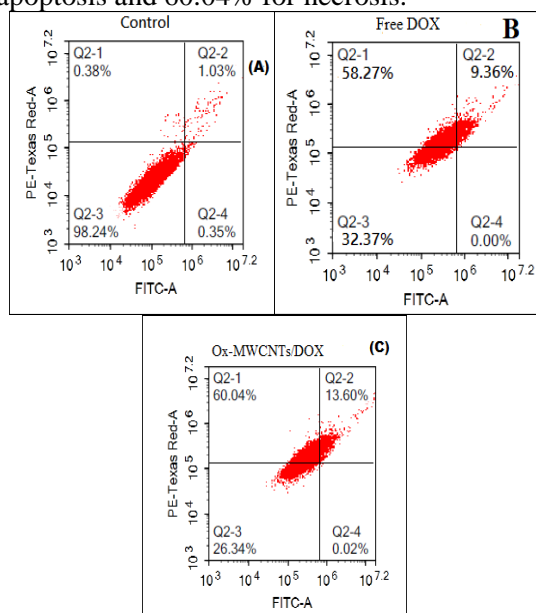


Figure 8: Histograms of apoptosis (A) Control cells, (B) treated cells with free DOX, (C) treated cells with Ox-MWCNTs/DOX.

Table 5: Percentages of cells distributions in apoptotic, necrotic and live stages

Stage	Control cells	Treated cells with free DOX	Treated cells with loaded DOX
Necrosis	0.38±0.022%	58.27±3.25 ^{sss1}	60.04±3.2 ^{sss1,s2}
Late apoptosis	1.03±0.04%	9.36±0.66 ^{sss1}	13.6±1.6 ^{sss1,ss2}
Live	98.24±1.1%	32.37±1.02 ^{sss1}	26.34±2.036 ^{sss1,s2}
Early apoptosis	0.35±0.011%	0.001±0.001 ^{sss1}	0.02±0.001 ^{sss1,n2}

Data represented as mean±SD where, Asterisks (s,ss,sss) indicates low significant, significant and highly significant, respectively while (n) not significant,¹ comparing to control cells and ² comparing to cells treated with free DOX

Discussion:

MWCNTs were used as the nanocarrier in our study. The carboxylic groups were added to their walls and ends using a functionalization process involving an acid mixture (nitric acid and sulfuric acid) (Lay *et al.*, 2010; Sharma *et al.*, 2010). This process was known as functionalization. The main goal of MWCNT functionalization was to increase hydrophilicity and dispersity in aqueous medium by adding hydrophilic groups (-COOH) (Singh *et al.*, 2017; Primastari *et al.*, 2022). The hydrophobic DOX solution was then mixed with the ox-MWCNTs nanoparticles, which were confirmed by FTIR, SEM, and We hypothesized that the MWCNTs' hollow structure provided a large area of surface, which aided in the trapping and containment of the DOX via - stacking and electrostatic interactions. As a result, the drug delivery system (DDS) had a large cargo capacity. As a result, MWCNT-based materials have a high potential for drug delivery (Yu *et al.*, 2016). The TEM images of OX-MWCNTs/DOX indicate that their tubular structure did not change, but they became darker and showed many smaller fragments. This is expected due to the loading of DOX, and these smaller fragments imply that MWCNTs were treated with DOX for longer periods of time under sonication and stirring, so MWCNTs were well dispersed and tended to be less aggregated in water. The latter findings lead one to use OX-MWCNTs/DOX as chemotherapeutic agent but after sonication for longer time to ensure their well dispersities in aqueous media; including

blood.

The morphological structure of Ox-MWCNTs/DOX from SEM differed slightly from that of Ox-MWCNT because they appeared to be more filled. This filling could be caused by DOX loading. The homogeneity and narrow particle size of the Ox-MWCNTs and Ox-MWCNTs/DOX were revealed by zeta size data. Furthermore, the particle size of Ox-MWCNTs/DOX increased after DOX loading. DOX encapsulation has been confirmed. The negative charge of Ox-MWCNTs indicated the success of the oxidation process as well as the presence of carboxylic and hydroxyl groups, which had previously been demonstrated using an FTIR spectrum.

The release behavior of DOX from Ox-MWCNTs/DOX *in vitro* under acidic pH 5.8 was found to be greater than that of the physiological environment. This could be because the hydrogen bond interaction between the Ox-MWCNT and doxorubicin is pH dependent. At pH 7.4, four hydrogen bonding possibilities were formed: (a) carboxylic group of MWCNT and hydroxyl group of DOX, (b) carboxylic group of MWCNT and amino group of DOX, (c) hydroxyl group of MWCNT and hydroxyl group of DOX, and (d) hydroxyl group of MWCNT and amino group of DOX (Huang *et al.*, 2011). Under acidic environment, pH 5.8, the amino groups of DOX are protonated, forming NH_3^+ , and thus unable to participate in hydrogen bonding. Moreover, in this acidic environment, the hydrogen proton in solution would compete with the group that form the hydrogen bond, weakening the previously described hydrogen bonding interaction, resulting in increased DOX release (Fabbro *et al.*, 2012). As a result, one can anticipate an increase in the retaining capacity of Ox-MWCNTs/DOX at physiological pH 7.4 and an improvement in the release of such cytotoxic drug in a tumour environment. Furthermore, the pH derangement in the tumour environment increases protonation of DOX amino groups, resulting in an increase in DOX solubility (Bi *et al.*, 2018). Additionally, increasing DOX solubility rises its tumorigenicity.

Using the SRB binding assay, the Ox-MWCNTs nanocarrier loaded DOX was tested for its *in vitro* cytotoxicity against MCF-7 and NBL cells. The cytotoxic effect of Ox-MWCNTs/DOX on MCF-7 and NBL cells was lower than that of free DOX, but it was greater

on MCF-7 than on NBL cells. These findings are correlated to the diverse metabolic rates of tumour and healthy cells, in addition to the different pH values of the two environments, because tumour cells are more energetic than normal cells, leading to an increase in the fermentation rate of glucose to produce lactic acid, which decreases the pH and effect on the DOX release, demonstrating that a slow release of the cytotoxic drug from the nano carrier system is associated with a decrease in load toxicity (Cirillo *et al.*, 2019). As effect of DOX released from Ox-MWCNTs/DOX on the viability of cancer cells was slightly lower than that of free DOX, this was also seen in our finding that 70% of the DOX was not released from the ox-MWCNTs even after 48hr or 60% was not released even after 7 days. These findings were consistent with those of other studies. According to the findings of (Cirillo *et al.*, 2019), the loaded MTX-CS-MWCNT were found to be discriminating in killing tumor cells, with unaffected viability of the healthy MRC-5 cells. Additionally, (Sharma *et al.*, 2017) discovered that the viability assay of DOX loaded on ox-DEX/PEG/MWCNTs decreased with concentration, while the percentage of cell viability of tumour cells decreased. According to the findings of (Ajima *et al.*, 2005), the effect of cisplatin released from CDDP@SWNHox on the viability of MCF-7 cancer cells was slightly lesser than that of free cisplatin.

The cell cycle in cancer cells is characterised by unrestrained proliferating and constant progression. As a result of any cell cycle phase regulation change, cancer cells reproduce rapidly. As a result, arresting the uncontrolled cell cycle at various stages is critical in cancer treatment (Yang *et al.*, 2018; Salazar *et al.*, 2016). In the current study, the cell cycle was studied *in vitro* on MCF-7 cells treated with free DOX and after its loading in an equivalent dose using the flow cytometric assay (Eivazi *et al.*, 2020). The cell cycle assay results showed that treating MCF-7 cells with free or loaded DOX reduces cell populations in the S phase while increasing them in the G1 and G2 phases for free DOX and decreasing them in the G2 phase for the loaded one. This could be because DOX caused DNA damage through DNA intercalation, free radical formation, or DNA double strand fragmentation. All of these factors work together to prevent DNA and RNA replication. As a result, the cell cycle is

stimulated to arrest or activate apoptosis-mediated cell death. DOX can also inhibit the topoisomerase II enzyme, which mediates DNA repair, causing DNA damage and inducing the apoptosis process (Zare *et al.*, 2019). These findings confirm that loaded DOX treatment increases both cellular apoptosis and necrosis more than free DOX treatment. These findings are consistent with those results acquired by (Ahmadi *et al.*, 2019), who discovered that the targeted delivery of DOX using pH sensitive poly lactided-co-glucolic acid-co-acrylic acid nanoparticles on GIT cancer HT-29 cell line encourages cellular arrest at the S and sub G1 phases.

Furthermore, MCF-7 cell death in the late apoptotic and necrotic stages is slightly improved after treatment with the loaded DOX compared to the free form. This finding confirms DNA fragmentation with a subsequent decrease in MCF-7 cell population in the G1 phase, possibly due to a disruption in DNA repair. This damage forces such tumour cell lines to undergo apoptosis (Ramasamy *et al.*, 2018; Rattanapornsompong *et al.*, 2021). In contrast, the MCF-7 cells treated with the free drug showed slightly lower cell accumulation in the late apoptotic and necrotic stages. This finding supports the role of MWCNTs in drug-induced apoptosis. Results were obtained in a somewhat similar manner by (Manatunga *et al.*, 2018). When DOX-loaded ALG-HI was used, their results revealed a greater cells percentage in both late apoptotic and necrotic stages. Furthermore, (Marina lyra *et al.*, 2021) discovered that treating with oxCNTs/GPEI25K carrier stimulates greater cell number in late apoptosis as well as necrosis, implying higher disruption of cell membrane integrity, most likely due to its high polymeric content. This content leads to increased drug internalization and, as a result, increased toxicity. The remarkable ability of the drug-loaded nanoparticles to induce apoptosis could result from increased in the nanoparticles uptake and subsequent flow of more drug into the nucleus.

Conclusion:

The drug delivery system (Ox-MWCNTs/DOX) was successfully prepared which were confirmed by different techniques as FTIR, SEM and TEM. The prepared Ox-

MWCNTs/DOX and free DOX were applied *in-vitro* on MCF-7 and NBL cell lines to study their cytotoxic effect and flowcytometric analysis (cell cycle and apoptosis). The loaded DOX showed much lower toxic effect on the normal cells (NBL cells) compared to the free one which is the aim of this study to avoid the side effects of free DOX on the normal cells with keeping its cytotoxic effects on the tumor ones.

References:

- Ahmedi, E., Zarghami, N., Jafarabadi, M. A., Alizadeh, L., Khojastehfard, M., Yamchi, M.R., & Salehi, R. (2019) Enhanced anticancer potency by combination chemotherapy of HT-29 cells with biodegradable, pH-sensitive nanoparticles for co-delivery of hydroxytyrosol and doxorubicin. In *Journal of Drug Delivery Science and Technology* (Vol. 51, pp. 721-735). Doi: 10.1016/j.jddst.2019.03.003
- Ajima, K., Yudasaka, M., Murakami, T., Maigne, T., Shiba, K., and Iijima, S. (2005). Carbon Nanohorns as Anticancer Drug Carriers. *Journal of MOLECULAR PHARMACEUTICS VOL. 2, NO. 6, 475-480* <https://doi.org/10.1021/mp0500566>
- Bi, J., Lu, Y., Dong, Y., & Gao, P. (2018). Synthesis of Folic Acid-Modified DOX@ZIF-8 Nanoparticles for Targeted Therapy of Liver Cancer. *Journal of Nanomaterials*, 2018(July), 1357812. Doi: 10.1155/2018/1357812
- Carvalho, C., Santos, R., X., Cardoso, S., Correia, S., Oliveira, P., J. Santos, M., S. & Moreira, P. I. (2009). Doxorubicin: The Good, the Bad and the Ugly Effect. *Current Medicinal Chemistry*, 16, 3267-3285 DOI: 10.2174/092986709788803312
- Chanphai, P., Thomas, T. J., & Tajmir-Riahi, H. A. (2019). Design of functionalized folic acid-chitosan nanoparticles for delivery of tetracycline, doxorubicin, and tamoxifen. *Journal of Biomolecular Structure and Dynamics*, 37(4), 1000-1006. Doi: 10.1080/07391102.2018.1445559
- Cirillo, G., Vittorio, O., Kunhardt, D., Valli, E., Voli, F., Farfalla, A., Curcio, M., Spizzirri U. G., and Hampel, S. (2019). Combining Carbon Nanotubes and Chitosan for the Vectorization of Methotrexate to Lung Cancer Cells. *Journal of Materials* 12, 2889; doi:10.3390/ma12182889
- Eivazi, N., Rahmani, R., & Paknejab, M. (2020). Specific cellular internalization and pH-responsive behavior of doxorubicin loaded pLGA-PEG nanoparticles targeted with anti EGFRvIII antibody. *Life Sciences*, 261(Nov),

118361. Doi: 10.1016/j.lfs.2020.118361
- Elhissi, A. M. A., Ahmed, W., Hassan, I. U., Dhanak, V. R., and D'Emanuele, A. (2011). Carbon Nanotubes in Cancer Therapy and Drug Delivery. *Journal of Drug Delivery*. Volume 2012, 10 pages doi:10.1155/2012/837327
- Fabbro, C., Boucetta, H. A., Ros, T. D., Kostarelos, K., Bianco, A., and Prato, M. (2012). Targeting carbon nanotubes against cancer. *Journal of The Royal Society of Chemistry Chem. Commun*, 48, 3911–3926 doi:10.1039/C2CC17995D
- Huang, H., Yuan, Q., Shah, J.S., Misra, R.D.K. (2011). A new family of folate-decorated and carbon nanotube-mediated drug delivery system: Synthesis and drug delivery response. *Journal of Advanced Drug Delivery Reviews* 63, 1332–1339 doi:10.1016/j.addr.2011.04.001
- Jain, N., Gupta, E., & Kanum N. J. (2022) Plethora of Carbon Nanotubes Applications in Various Fields – A State-of-the-Art-Review. (2022). SMART SCIENCE <https://doi.org/10.1080/23080477.2021.1940752>
- Kumari, M., Purohit, M.P., Patnaik, S., Shukla, Y., Kumar, P., & Gupta, K.C. (2018). Curcumin loaded selenium nanoparticles synergize the anticancer potential of doxorubicin contained in self-assembled, cell receptor targeted nanoparticles. *European Journal of Pharmaceutics and Biopharmaceutics*, 130 (Sep), 185-199. Doi: 10.1016/j.ejpb.2018.06.030
- Lay, C. L., Liu, H. Q., Tan, H. R., and Liu, Y. (2010). Delivery of paclitaxel by physically loading onto poly (ethylene glycol) (PEG)-graft carbon nanotubes for potent cancer therapeutics. *Journal of Nanotechnology* 21, 065101 (10pp) doi:10.1088/0957-4484/21/6/065101
- Lyra, K. M., Kaminari, A., Panagiotaki, K. N., Spyrou, K., Papageorgiou, S., Sakellis, E., Katsaros, F. K., and Sideratou, Z. (2021). Multi-Walled Carbon Nanotubes Decorated with Guanidinylated Dendritic Molecular Transporters: An Efficient Platform for the Selective Anticancer Activity of Doxorubicin. *Journal of Pharmaceutics* 2021, 13, 858. <https://doi.org/10.3390/pharmaceutics13060858>
- Manatunga, D. C., Silva, R. M., Silva, K. M. N., Malavige, G. N., Wijeratne, D. T., Williams, G. R., Jayasinghe, C. D., Udagama, B. V. (2018). Effective delivery of hydrophobic drugs to breast (MCF-7) and Liver (HepG2) cancer cells: A detailed investigation using Cytotoxicity assays, fluorescence imaging and flow cytometry. *European Journal of Pharmaceutics and Biopharmaceutics*. <https://doi.org/10.1016/j.ejpb.2018.04.001>
- Primastari, S. D., Kusumastuti, Y., Handayani, M., Rochmadi. (2022). Functionalization of multi-walled carbon nanotube (MWCNT) with CTACe surfactant and polyethylene glycol as potential drug carrier. *Earth and Environmental Science* 963 (2022) 012033 doi:10.1088/1755-1315/963/1/012033
- Qi, X., Rui, Y., Fan, Y., Chen, H., Ma, N., Wu, Z. (2015). Galactosylated chitosan-grafted multiwall carbon nanotubes for pH-dependent sustained release and hepatic tumor-targeted delivery of doxorubicin in vivo. *Journal of Colloids and Surfaces B: Biointerfaces* 133, 314–322 <http://dx.doi.org/10.1016/j.colsurfb.2015.06.003>
- Ramasamy, T., Ruttala, H. B., Sundaramoorthy, P., Poudel, B. K., Youn, Y. S., Ku, S. K., Choi, H.-G., Yong, C. S., & Kim, J.O. (2018). Multimodal selenium nanoshell-capped Au@mSiO₂ nanoplatforam for NIR-responsive chemophotothermal therapy against metastatic breast cancer. *NPG Asia Materials*, 10(4), 197-216. Doi: 10.1038/s41427-018-0034-5
- Rattanapornsompong, K., Khatiya, J., Phannasil, P., Phaoakrop, N., Roytrakul, S., Jitrapakdee, S., & Akekawatchai, C. (2021). Impaired G2/M cell cycle arrest induces apoptosis in pyruvate carboxylase knockdown MDA-MB-231 cells. *Biochemistry and Biophysics Reports*, 25(March), 100903. Doi: 10.1016/j.bbrep.2020.100903
- Rivankar, S. (2014). An overview of doxorubicin formulations in cancer therapy. *Journal of Cancer Research and Therapeutics - October-December 2014 - Volume 10 - Issue 4 DOI: 10.4103/0973-1482.139267*
- Salazar-roa, M., & Malumbres, M. (2016). Fueling the Cell Division Cycle. *Trends in Cell Biology*, 27(1), 69-81. Doi: 10.1016/j.tcb.2016.08.009
- Sharma, P., Jain, K., Jain, N.K., Mehra, N. K. (2017). Ex vivo and in vivo performance of anti-cancer drug loaded carbon nanotubes. *Journal of Drug Delivery Science and Technology* 41, 134-143 <http://dx.doi.org/10.1016/j.jddst.2017.07.011>
- Sheikhpour, M., Golbabaie, A., & Kasaeian, A., (2017) Carbon nanotubes: A review of novel strategies for cancer diagnosis and treatment. *Materials Science and Engineering C* 76 1289–1304 <http://dx.doi.org/10.1016/j.msec.2017.02.132>
- Singh, R. P., Sharma, G., Sonali, Singh, S., Bharti, S., Pandey, P. L., Koch, B., Muthu, M. S. (2017). Chitosan-folate decorated carbon nanotubes for site specific lung cancer delivery. *Journal of Materials Science & Engineering C* doi: 10.1016/j.msec.2017.03.225
- WANG, J.-J., LEI, K.-F., & HAN, F. (2018). Tumor

- microenvironment: recent advances in various cancer treatments. *European Review for Medical and Pharmacological Sciences*, 22: 3855-3864 doi: 10.26355/eurrev_201806_15270.
- Wu, T. C., Lee, P. Y., Lai, C.L., & lai, C. H. (2021). Synthesis of Multi-Functional Nano-Vectors for Targeted-Specific Drug Delivery. *Polymers*, 13(3), 451-464. Doi: 10.3390/polym13030451
- Yang, V. W. (2018). *The Cell Cycle*. In *Physiology of the Gastrointestinal Tract (Sixth Edit)*. Elsevier Inc. doi:10.1016/B978-0-12-809954-4.00008-6
- Yu, B., Tan, L., Zheng, R., Tan, H., Zheng, L. (2016). Targeted delivery and controlled release of Paclitaxel for the treatment of lung cancer using single-walled carbon nanotubes. *Journal of Materials Science and Engineering C* 68 , 579–584
http://dx.doi.org/10.1016/j.msec.2016.06.025
- Zare, M. F. R., Rakhshan, K., Aboutaleb, N., Nikbakht, F., Naderi, N., Bakhshesh, M., & Azizi, Y. (2019). Apigenin attenuates doxorubicin induced cardiotoxicity via reducing oxidative stress and apoptosis in male rats. *Life Sciences*, 232(July), 116623. Doi: 10.1016/j.lfs.2019.116623.

الملخص العربي

عنوان البحث: التحضير والتطبيقات المخبرية للدوكسوروبيسين المحملة على أنابيب نانوية كربونية متعددة الجدران

الشحات طوسون^١، نورهان رزق^١، رشازهران^١
^١ قسم الكيمياء - كلية العلوم - جامعة دمياط - دمياط الجديدة - مصر

تعد أنابيب الكربون النانومترية متعددة الجدران (MWCNTs) واحدة من أهم المواد النانومترية لمختلف التطبيقات الطبية الحيوية. حيث يمكن استخدامها لتوصيل مختلف العقاقير إلى أماكن الورم المستهدفة، بما في ذلك دوكسوروبيسين (DOX). وذلك لأن MWCNTs يمكن أن تخترق الأغشية البيولوجية مسببة سمية خلوية منخفضة. في هذه الدراسة، تم تحسين MWCNTs عن طريق الأكسدة (Ox-MWCNTs) لتحسين قابليتها للذوبان والتوافق الحيوي. ومن ثم تم اختبار قدراتها على حمل عقار DOX (Ox-MWCNT / DOX). وبعد ذلك تم تمييز هذه الجسيمات باستخدام FTIR و TEM و SEM و zeta size كما تم تقييم أنشطتهم المضادة للورم ضد الخلايا المخبرية MCF-7 و NBL. وقد أكدت نتائج FTIR إضافة مجموعات الكربوكسيل إلى MWCNTs متبوعاً بتحميل DOX وكان شكلها أنبوبياً بنهايات مفتوحة باستخدام TEM. كما بدت الأنابيب من السطح، وكانت كرات مجوفة ذات هيكل مترابط، باستخدام SEM. كما لوحظ ارتفاع معدل إطلاق DOX عند الأس الهيدروجيني ٨، مقارنة بالرقم الهيدروجيني الفسيولوجي. كما أدى علاج خلايا (MCF-7) باستخدام Ox-MWCNT / DOX إلى بقاء حيوية الخلايا بمقدار 96 ± 0.37 ، 87 ± 0.7 ، 34.7 ± 0.75 ، 14.3 ± 1 و 4.2 ± 0.5 ٪ بجرعات تعادل ١، ١٠، ١٠٠ و ١٠٠٠ ميكروغرام / مل من دوكس، على التوالي. علاوة على ذلك، لوحظت حيوية أعلى (99.8 ± 0.13 ، 99.54 ± 0.69 ، 77.42 ± 1.13 ، 62.48 ± 0.1 و 55.3 ± 1.25 ٪) مع انخفاض سمية خلايا الطبيعية (NBL) بموجب بروتوكول العلاج نفسه. لذلك، قد يكون بروتوكول التحميل هذا واعدًا لعلاج هذا النوع من الورم بعد إجراء مزيد من الدراسات في المستقبل.